A TENSOR MODEL FOR NEMATIC PHASES OF BENT-CORE MOLECULES BASED ON MOLECULAR THEORY[*]

JIE XU[†], FANGFU YE[‡], AND PINGWEN ZHANG[§]

Abstract. We construct a tensor model for nematic phases of bent-core molecules from molecular theory. The form of free energy is determined by molecular symmetry, which includes the couplings and derivatives of a vector and two second-order tensors, with the coefficients determined by molecular parameters. We use the model to study the nematic phases resulting from the hard-core potential. Unlike most macroscopic models, we are able to obtain the phase diagram about the molecular parameters, but not merely some phenomenological coefficients. The tensor model is applicable to other molecules with the same symmetry, which we demonstrate by studying the phase diagram of star molecules.

Key words. liquid crystals, bent-core molecules, tensor model, molecular theory, modulated nematic phases, twist-bend phase

AMS subject classifications. 76A15, 82D30

DOI. 10.1137/16M1099789

1. Introduction. The ability to show complex orientational order has drawn much attention from the liquid crystal community to bent-core molecules. This feature originates from the C_{2v}[1] molecular symmetry that breaks the axisymmetry of a rod-like molecule. The polar and biaxial order is notable in layer or columnar structures [8, 31]. The homogeneous biaxial nematic phase is also observed [20, 1], spontaneously formed by bent-core molecules without imposing external forces. Moreover, bent-core molecules are able to exhibit modulated nematic phases that have constant number density in space but show modulation in orientational distribution. The prediction was made very early [22, 10]. Later, the twist-bend phase was identified experimentally [27, 11, 26, 24, 5, 7].

The modulated nematic phases have also been discussed theoretically with different macroscopic phenomenological models [19, 30, 33, 34, 29]. They are helpful in understanding the phase behaviors. However, since these models focus on particular phase transitions only, the order parameters and terms in the free energy are incomplete. In particular, all of these models do not include the biaxial nematic phase, which is studied separately in the literature (see [4] and the references therein). Also, these models provide little information about the effect of molecular interaction on the phase transition. Some models incorporate microscopic interaction [13, 32], but the desired phases are induced under artificial external forces that resemble the struc-

[†]LMAM & School of Mathematical Sciences, Peking University, Beijing 100871, China. Current address: Department of Mathematics, Purdue University, West Lafayette, IN 47907 (rxj_2004@126.com).

[‡]Beijing National Laboratory for Condensed Matter Physics, Institute of Physics, Chinese Academy of Sciences, Beijing 100090, China, and School of Physical Sciences, University of Chinese Academy of Sciences, Beijing 100094, China (fye@iphy.ac.cn).

[§]Corresponding author. LMAM & School of Mathematical Sciences, Peking University, Beijing 100871, China (pzhang@pku.edu.cn).

[1]This is the Schönflies notation.

ture of the phases. On the other hand, molecular simulations [6, 23, 17, 9, 25] have also been carried out for bent-core molecules. A recent work [12] uses both molecular theory and molecular simulation to study a curved molecule that can exhibit the twist-bend phase. Molecular theory or molecular simulation can, indeed, build a connection between molecular interaction and phase behaviors, but they are also costly in computation.

Understanding the connection between the molecular interaction and the resulting phase behaviors is the fundamental problem for liquid crystals. It is more significant for bent-core molecules because ample experimental results suggest that the phase behaviors of bent-core molecules can be sensitively dependent on specific molecular architecture [31]. To achieve this goal, it is necessary that we are armed with a model that (1) clearly reflects the role of molecular interaction and that (2) can be solved efficiently, so that we can systematically examine the effect of physical parameters without spending a very long time. Of all the models we mentioned above, microscopic models only meet the first requirement, while macroscopic models only meet the second, although some efforts are made to match both goals [16, 28].

In [14], a tensor model is constructed for rod-like molecules, which takes a macroscopic form, while carrying information of the microscopic interaction. Starting from the molecular theory that includes the entropy and the pairwise interaction, the model is derived by the expansion of the spatial moments of the kernel function, along with the Bingham approximation [3] that minimizes the entropy term with the value of the second-order tensor fixed. By adopting the hard-core interaction and a simple molecular geometry, analytical calculations can be done in the expansion. In the resulting model, the free energy is expressed by some tensors, with the coefficients being functions of molecular parameters.

For general cases where analytical calculations are not available, we have discussed the expansion for homogeneous phases [35]. First, we analyze the symmetries of the spatially homogeneous kernel function that originate from the molecular symmetry. Then, we are able to choose a finite-dimensional polynomial space satisfying the symmetries. Since we can separate variables for each monomial, the free energy can be expressed by some tensors if we use any function in the polynomial space to approximate the kernel function. When the truncation criterion is fixed, the polynomial space is determined by the symmetries. Therefore, the form of free energy, as well as the tensors that appear in the free energy and serve as order parameters, is determined by molecular symmetry. For bent-core molecules, if we truncate at second order, the order parameters include three tensors, one first order and two second order. Finally, we calculate the projection of the kernel function in the polynomial space to derive the coefficients. In this way, the coefficients receive the information of molecular interaction in the kernel function and are expressed as functions of molecular parameters.

The purpose of this paper is to construct a tensor model for inhomogeneous phases. Now the kernel function is not spatially homogeneous, so we need to approximate its spatial moments as in [14]. In this case, the procedure for spatially homogeneous phases is still applicable with significant extensions technically. In particular, we need to find a suitable representation of spatial moments before writing down the approximation polynomial space. The resulting free energy is still a functional of the three tensors obtained for the homogeneous phases but contains couplings and derivatives that enable us to study modulated nematic phases. For the entropy term, we follow the idea for rod-like molecules by minimizing it with the value of three tensors fixed. The model has the following features.
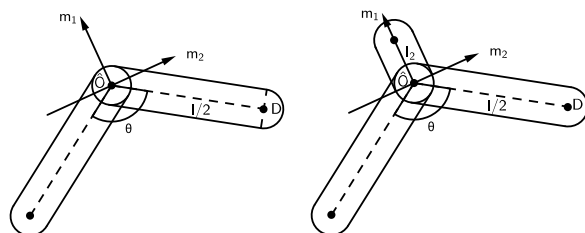
FIG. 1. *A bent-core molecule (left) and a star molecule (right).*

- The form of free energy is determined by the molecular symmetry. Thus, the model is applicable to any molecule with the same symmetry. Moreover, the free energy is independent of the choice of the reference space-fixed orthonormal frame.
- Under a certain truncation criterion, the model includes all the terms allowed by the molecular symmetry. Thus, the model is not specifically designed for certain phase transitions.
- For molecules with the same symmetry and different architecture or interaction, they are differentiated by the coefficients that are derived as functions of molecular parameters.
- As a special case, the model reduces to a model for rod-like molecules if the bending is straightened.

We use the model to study the nematic phases of bent-core molecules resulting from the hard-core interaction and find that the uniaxial and biaxial nematic phases, as well as the modulated twist-bend phase, can possibly occur, which cover all the nematic phases found experimentally so far. We obtain the phase diagram about molecular parameters, showing how the molecular parameters affect the modulation in the twist-bend phases. In addition, we examine the nematic phases of star molecules, a variant of bent-core molecules, to illustrate the effect of the molecular shape on the phase behavior. To our knowledge, it is the first result in which the phase behavior about the molecular shape is systematically examined in a theoretical model.

The rest of paper is organized as follows. In section 2, we derive the tensor model from molecular theory. The numerical results are presented in section 3. A concluding remark is given in section 4. Some details are given in Appendices A and B.

2. The tensor model.

2.1. Notation. We consider bent-core molecules and star molecules, drawn in Figure 1. A bent-core molecule has two identical arms jointed with fixed angle θ. Each arm is a cylinder with two spherical caps, with the length $l/2$ and the diameter D. A star molecule has a third arm of the length l_2 along the arrowhead direction. Both molecules are regarded as fully rigid. Thus, the position and orientation of a molecule are represented by those of the orthonormal frame $(\hat{O}; \boldsymbol{m}_1, \boldsymbol{m}_2, \boldsymbol{m}_3)$ mounted on it. As shown in Figure 1, $\boldsymbol{m}_1$ points toward the arrowhead direction, and $\boldsymbol{m}_2$ is along the connection of the farther ends of two arms. Both molecules have the C_{2v} symmetry, which allows the symmetry plane $\hat{O}\boldsymbol{m}_1\boldsymbol{m}_2$ and the twofold rotational symmetry round $\boldsymbol{m}_1$. Denote by $\boldsymbol{x} \in \mathbb{R}^3$ the position of $\hat{O}$ and by $P \in SO(3)$ the orientation of the frame. The matrix representation of P, which consists of the components of $\boldsymbol{m}_i$, can

be expressed by Euler angles,

(2.1)

$$
P = (\boldsymbol{m}_1, \boldsymbol{m}_2, \boldsymbol{m}_3) = \left(\begin{array}{ccc} m_{11} & m_{21} & m_{31} \\ m_{12} & m_{22} & m_{32} \\ m_{13} & m_{23} & m_{33} \end{array} \right)
$$

$$
= \left(\begin{array}{ccc} \cos\alpha & -\sin\alpha\cos\gamma & \sin\alpha\sin\gamma \\ \sin\alpha\cos\beta & \cos\alpha\cos\beta\cos\gamma - \sin\beta\sin\gamma & -\cos\alpha\cos\beta\sin\gamma - \sin\beta\cos\gamma \\ \sin\alpha\sin\beta & \cos\alpha\sin\beta\cos\gamma + \cos\beta\sin\gamma & -\cos\alpha\sin\beta\sin\gamma + \cos\beta\cos\gamma \end{array} \right).
$$

The uniform probability measure on $SO(3)$ is given by

$$
\mathrm{d}P = \frac{1}{8\pi^2} \sin\alpha \mathrm{d}\alpha \mathrm{d}\beta \mathrm{d}\gamma.
$$

We can also view $\boldsymbol{m}_i$ and m_{ij} as functions of P. In what follows, we use the notation $\boldsymbol{m}_i(P)$ and $m_{ij}(P)$ to represent the $\boldsymbol{m}_i$ and m_{ij} determined by a certain P.

The summation over repeated indices will be used. The product $\boldsymbol{m}_1\boldsymbol{m}_1$ is recognized as the tensor product and results in a second-order tensor, while $\boldsymbol{m}_1 \cdot \boldsymbol{m}_2$ is the inner product. For a second-order tensor Q, we use $|Q|^2 = Q : Q = Q_{ij}Q_{ij}$.

2.2. The derivation of tensor model. Our starting point is the second virial expansion. The free energy includes the entropy and the contribution of pairwise molecular interaction,

(2.2)
$$
\frac{F[f]}{\beta_0} = \int \mathrm{d}P\mathrm{d}\boldsymbol{x} f(\boldsymbol{x}, P) \log f(\boldsymbol{x}, P) + \frac{1}{2} \int \mathrm{d}P\mathrm{d}\boldsymbol{x}\mathrm{d}P'\mathrm{d}\boldsymbol{x}' f(\boldsymbol{x}, P) G(\boldsymbol{r}, P, P') f(\boldsymbol{x}', P'),
$$

where $\boldsymbol{r} = \boldsymbol{x}' - \boldsymbol{x}$ is the relative position of two molecules. The energy is measured by β_0, the product of the Boltzmann constant and the temperature. The number density f is a function of the position $\boldsymbol{x}$ and the orientation P. We define $c(\boldsymbol{x}) = \int \mathrm{d}P f(\boldsymbol{x}, P)$ as the spatial concentration and $\rho(\boldsymbol{x}, P) = f(\boldsymbol{x}, P)/c(\boldsymbol{x})$ as the orientational density. They satisfy

$$
\int \mathrm{d}\boldsymbol{x}\mathrm{d}P f(\boldsymbol{x}, P) = \int \mathrm{d}\boldsymbol{x} c(\boldsymbol{x}) \int \mathrm{d}P \rho(\boldsymbol{x}, P) = c_0 V,
$$

where V is the volume of the system, and c_0 is the average concentration. The kernel $G(\boldsymbol{r}, P, P')$ is the Mayer function $G = 1 - \exp(-U/\beta_0)$ [21] about the pairwise potential U. In the case of hard-core potential, if two molecules touch, then $U(\boldsymbol{r}, P, P') = +\infty$, leading to $G(\boldsymbol{r}, P, P') = 1$; otherwise, $U(\boldsymbol{r}, P, P') = 0$, namely $G(\boldsymbol{r}, P, P') = 0$.

To derive the form of the tensor model, we expand the pairwise interaction term in (2.2) about $\boldsymbol{r}$ and P. After the expansion, we are able to express the pairwise interaction term by the three tensors identified in [35]. Then, we minimize the entropy term with the value of these tensors fixed, so that it is also expressed as a functional of the three tensors. This approach has also been adopted for rod-like molecules [2, 15, 14], where the density function becomes the Bingham distribution.

2.2.1. Spatial and orientational expansion. First, we do Taylor expansion on $f(\boldsymbol{x}', P') = f(\boldsymbol{x} + \boldsymbol{r}, P')$ with respect to $\boldsymbol{r}$, yielding

(2.3)
$$
\frac{F[f]}{\beta_0} = \int \mathrm{d}P\mathrm{d}\boldsymbol{x} f(\boldsymbol{x}, P) \log f(\boldsymbol{x}, P)
$$
$$
+ \sum_{k \geq 0} \frac{1}{2k!} \int \mathrm{d}\boldsymbol{x}\mathrm{d}P\mathrm{d}P' f(\boldsymbol{x}, P) M^{(k)}(P, P') \nabla^k f(\boldsymbol{x}, P'),
$$

where

$$(2.4) \qquad M^{(k)}(P, P') = \int G(\boldsymbol{r}, P, P') \underbrace{\boldsymbol{r} \dots \boldsymbol{r}}_{k \text{ times}} \, \mathrm{d}\boldsymbol{r},$$

a kth-order symmetric tensor, is the kth moment of G. For the hard-core interaction, the integration is taken on the region where $G = 1$. By determining this region, we are able to calculate $M^{(k)}$ numerically. The details are described in Appendix A. Because the size of the region is proportional to l^3, we have $M^{(k)} \propto l^{k+3}$.

Next, we expand $M^{(k)}(P, P')$ with respect to P and P'. To clearly present the idea, we briefly review the expansion of $M^{(k)}$ for rod-like molecules discussed in [14]. In particular, we only look at $M^{(0)}$ and $M^{(2)}$ because they are sufficient for nematic phases (note that $M^{(1)} = 0$). In this case, $M^{(k)} = M^{(k)}(\boldsymbol{m}, \boldsymbol{m}')$, where $\boldsymbol{m}$ and $\boldsymbol{m}'$ are the directors of two rods (or, in the context of the current work, we may let $\boldsymbol{m} = \boldsymbol{m}_1(P)$ and $\boldsymbol{m}' = \boldsymbol{m}_1(P')$; see Theorem 3.4 in [35]). Analytical calculations give

$$(2.5) \qquad M^{(0)}(\boldsymbol{m}, \boldsymbol{m}') = M^{(0)}(\eta),$$

$$(2.6) \qquad M^{(2)}(\boldsymbol{m}, \boldsymbol{m}') = B_1(\eta)I + B_2(\eta)(\boldsymbol{mm} + \boldsymbol{m}'\boldsymbol{m}') + B_3(\eta)(\boldsymbol{mm}' + \boldsymbol{m}'\boldsymbol{m}),$$

where $\eta = \boldsymbol{m} \cdot \boldsymbol{m}'$ is the inner product of the two directors, and I is the identity matrix. Then, $M^{(0)}(\eta)$ and $B_i(\eta)$ are expanded as polynomials of η. In the resulting approximation formulas, $M^{(0)}$ and $M^{(2)}$ are expressed as polynomials of $\boldsymbol{m}$ and $\boldsymbol{m}'$. In this way, the variables $\boldsymbol{m}$ and $\boldsymbol{m}'$ are separated, leading to the approximate free energy as a function of tensors. An important point to be noted is the truncation of $M^{(0)}(\eta)$ and $B_i(\eta)$. The truncation is according to the order of each of $\boldsymbol{m}$ and $\boldsymbol{m}'$. Specifically, $M^{(0)}$ and B_1 are truncated at fourth order, B_2 at second order, and B_3 at third order. This is because $\boldsymbol{mm} + \boldsymbol{m}'\boldsymbol{m}'$ contribute to the order by two, and $\boldsymbol{mm}' + \boldsymbol{m}'\boldsymbol{m}$ contribute to the order by one. By this truncation, the approximation formulas include all the terms such that each of $\boldsymbol{m}$ and $\boldsymbol{m}'$ is not larger than fourth order, respectively. This truncation is adopted because the order of $\boldsymbol{m}$ and $\boldsymbol{m}'$ determines the order of tensor in the free energy. Under the above truncation, the corresponding free energy is a function including all the allowed terms of tensors up to fourth order.

Returning to bent-core molecules, we aim to approximate each component of $M^{(k)}$ as a polynomial of $\boldsymbol{m}_j(P)$ and $\boldsymbol{m}'_j = \boldsymbol{m}_j(P')$. Similar to rod-like molecules [14], we will only consider $k = 0, 1, 2$ because we only examine nematic phases. Since we cannot do analytical calculations, we will follow the procedure in [35] with some extensions to determine the form of approximation formula by symmetric properties. The case $k = 0$ has been discussed previously and will be reviewed shortly. For $k \geq 1$, we will first write down expressions similar to (2.6), followed by polynomial approximations. For the truncation of the polynomials, we only retain the terms such that the degrees of $\boldsymbol{m}_j$ and $\boldsymbol{m}'_j$ are no more than second order, respectively. This makes the free energy as a function of tensors up to second order. The choice is largely based on keeping the model concise. One can also choose to truncate at fourth order like what is done for rod-like molecules, but at the expense of having over 100 terms in the free energy.

Denote the relative orientation and its components as

$$(2.7) \qquad \bar{P} = P^{-1}P' = (p_{ij})_{3\times 3} = (\boldsymbol{m}_i \cdot \boldsymbol{m}'_j)_{3\times 3}, \quad i, j = 1, 2, 3,$$

where we denote $\boldsymbol{m}'_i = \boldsymbol{m}_i(P')$. The following equalities shall be satisfied for molecules with the symmetry plane $\hat{O}\boldsymbol{m}_1\boldsymbol{m}_2$:

$$(2.8) \qquad G(T\boldsymbol{r}, TP, TP') = G(\boldsymbol{r}, P, P') \quad \forall T \in SO(3),$$

$$(2.9) \qquad G(-\boldsymbol{r}, P', P) = G(\boldsymbol{r}, P, P'),$$

$$(2.10) \qquad G(-\boldsymbol{r}, PJ, P'J) = G(\boldsymbol{r}, P, P') \text{ for } J = \operatorname{diag}(-1, -1, 1).$$

The above equalities have been stated in [35]. The meaning of the three equalities is that G is invariant when two molecules rotate together, when two molecules are switched, and when one molecule is reflected about the plane $\hat{O}\boldsymbol{m}_1\boldsymbol{m}_2$ of the other molecule.

As the simplest case, we review the key points in the expansion of $M^{(0)}$. By setting $T = P^{-1}$ in (2.8), we can see that $M^{(0)}(P, P') = M^{(0)}(I, P^{-1}P')$. Thus, $M^{(0)}$ is a function of the relative orientation $\bar{P}$. Then, from (2.10), we deduce that

$$(2.11) \qquad M^{(0)}(\bar{P}) = M^{(0)}(J\bar{P}J).$$

Note that $\bar{P}$ and $J\bar{P}J$ are the only two elements in $SO(3)$ when $(p_{11}, p_{12}, p_{21}, p_{22})$ is fixed. Hence $M^{(0)}$ is reduced to a function of the above four scalars. By (2.9), we have $M^{(0)}(\bar{P}) = M^{(0)}(\bar{P}^T)$, leading to

$$(2.12) \qquad M^{(0)}(p_{11}, p_{12}, p_{21}, p_{22}) = M^{(0)}(p_{11}, p_{21}, p_{12}, p_{22}).$$

We use a polynomial of p_{11}, p_{12}, p_{21}, p_{22} to approximate $M^{(0)}$, denoted by $\hat{M}^{(0)}$. It shall satisfy (2.12) as well. Furthermore, it has the $\boldsymbol{m}_2 \to -\boldsymbol{m}_2$ and $\boldsymbol{m}'_2 \to -\boldsymbol{m}'_2$ symmetries. Since $p_{ij} = \boldsymbol{m}_i \cdot \boldsymbol{m}'_j$, only the terms where both $\boldsymbol{m}_2$ and $\boldsymbol{m}'_2$ appear even times can be retained. For example, the term $p_{22} = \boldsymbol{m}_2 \cdot \boldsymbol{m}'_2$ will be discarded since both $\boldsymbol{m}_2$ and $\boldsymbol{m}'_2$ appear one time. Thus, we obtain the following quadratic approximation:

$$(2.13) \qquad \hat{M}^{(0)} = c_{00} + c_{01}p_{11} + c_{02}p_{11}^2 + c_{03}p_{22}^2 + c_{04}(p_{12}^2 + p_{21}^2).$$

The first index of the coefficients c_{0j} is zero, corresponding to the zeroth moment $M^{(0)}$. These coefficients are independent of P and P'.

When we apply the above procedure to the expansion of $M^{(k)}$ for $k \geq 1$, some modifications need to be made since $M^{(k)}$ is a kth-order tensor. We will first seek a representation similar to (2.6). The representation (2.6) conveys two messages:

1. $M^{(2)}$ can be expressed as a linear combination of some tensors generated by $\boldsymbol{m}$ and $\boldsymbol{m}'$ and I. Moreover, the expression is symmetric about $\boldsymbol{m}$ and $\boldsymbol{m}'$.
2. The coefficients B_i depend only on $\boldsymbol{m} \cdot \boldsymbol{m}'$, which describes the relative orientation of $\boldsymbol{m}$ and $\boldsymbol{m}'$.

Actually, these two statements hold for any $M^{(k)}$ (see (3.22) in [14] for the fourth moment $M^{(4)}$). With this observation, for bent-core molecules, we first seek a representation of $M^{(k)}$ by a linear combination of tensors generated by $\boldsymbol{m}_i(P)$, $\boldsymbol{m}'_i = \boldsymbol{m}_i(P')$, and I, which is symmetric about P and P'. Then, we figure out the symmetry of the coefficients in this representation, followed by the polynomial approximation. We pay particular attention to the effect of the symmetry plane $\hat{O}\boldsymbol{m}_1\boldsymbol{m}_2$. It eliminates the appearance of $\boldsymbol{m}_3$ and $\boldsymbol{m}'_3$ in $M^{(0)}$ by (2.11). We can also eliminate them in any $M^{(k)}$, as we will show below. We will only discuss $M^{(1)}$ in detail because $M^{(2)}$ follows the same way.

Now we start to discuss $M^{(1)}$.

Step 1. We show that for fixed (P, P'), $M^{(1)}$ can be expressed as

$$(2.14) \qquad M^{(1)}(P, P') = \tilde{c}_1 \boldsymbol{m}_1 + \tilde{c}_2 \boldsymbol{m}_2 + \tilde{c}_{1'} \boldsymbol{m}_1' + \tilde{c}_{2'} \boldsymbol{m}_2',$$

where $\tilde{c}_j$ $(j = 1, 2, 1', 2')$ are functions of (P, P').

We begin with writing

$$(2.15) \qquad M^{(1)}(P, P') = \tilde{c}_1 \boldsymbol{m}_1 + \tilde{c}_2 \boldsymbol{m}_2 + \tilde{c}_3 \boldsymbol{m}_3.$$

To write down a representation symmetric about P and P', we express $\boldsymbol{m}_3$ by a linear combination of $\boldsymbol{m}_1$, $\boldsymbol{m}_2$, $\boldsymbol{m}_1'$, and $\boldsymbol{m}_2'$. Note that this cannot be done when $\boldsymbol{m}_3 = \pm \boldsymbol{m}_3'$ because in this case span$\{\boldsymbol{m}_1, \boldsymbol{m}_2, \boldsymbol{m}_1', \boldsymbol{m}_2'\}$ = span$\{\boldsymbol{m}_1, \boldsymbol{m}_2\}$, and $\boldsymbol{m}_3 \notin$ span$\{\boldsymbol{m}_1, \boldsymbol{m}_2\}$. However, if the molecule has the symmetry plane $\hat{O}\boldsymbol{m}_1\boldsymbol{m}_2$, we show that $\tilde{c}_3 = 0$ when $\boldsymbol{m}_3 = \pm \boldsymbol{m}_3'$. Actually, the condition $\boldsymbol{m}_3 = \pm \boldsymbol{m}_3'$ can be rewritten as $\bar{P} = P^{-1}P' = \text{diag}(W, \pm 1)$, where W is a 2×2 orthogonal matrix. Thus, we have $J\bar{P}J = \bar{P}$, with $J = \text{diag}(-1, -1, 1)$. Together with (2.8) and (2.10), we have

$$(2.16) \qquad G(\boldsymbol{r}, P, P') = G(P^{-1}\boldsymbol{r}, I, \bar{P}) = G(-P^{-1}\boldsymbol{r}, J, \bar{P}J)$$
$$= G(-JP^{-1}\boldsymbol{r}, I, J\bar{P}J) = G(-JP^{-1}\boldsymbol{r}, I, \bar{P}) = G(-PJP^{-1}\boldsymbol{r}, P, P').$$

Note that $-PJP^{-1}\boldsymbol{r} = \boldsymbol{r} - 2(\boldsymbol{r} \cdot \boldsymbol{m}_3)\boldsymbol{m}_3$. Taking (2.16) into (2.4), we obtain

$$(2.17) \qquad 2\tilde{c}_3 = 2\boldsymbol{m}_3 \cdot M^{(1)}(P, P') = 2 \int G(\boldsymbol{r}, P, P')(\boldsymbol{r} \cdot \boldsymbol{m}_3)\mathrm{d}\boldsymbol{r}$$
$$= \int \left(G(\boldsymbol{r}, P, P') + G(-PJP^{-1}\boldsymbol{r}, P, P')\right)(\boldsymbol{r} \cdot \boldsymbol{m}_3)\mathrm{d}\boldsymbol{r}$$
$$= \int G(\boldsymbol{r}, P, P')(\boldsymbol{r} - PJP^{-1}\boldsymbol{r}) \cdot \boldsymbol{m}_3 \mathrm{d}\boldsymbol{r}$$
$$= 0.$$

Therefore, when the molecule has the symmetry plane $\hat{O}\boldsymbol{m}_1\boldsymbol{m}_2$, we are allowed to use the representation (2.14).

Remark. Whether the molecular has a symmetry plane affects the form of the representation of $M^{(k)}$. If the molecule is chiral, we have to include $\boldsymbol{m}_3$. It is also the case for rod-like molecules. Actually, we have $M^{(1)} \neq 0$ even if a chiral rod-like molecule has the head-to-tail symmetry.

Step 2. We analyze the symmetric properties of the scalars $\tilde{c}_j$ in (2.14). Apparently, the representation (2.14) is not unique. In what follows, when we say that $\tilde{c}_j$ satisfy certain symmetries, it means that there exists a representation in which the symmetries hold.

First, we can require that they are functions of $\bar{P}$. We deduce from (2.8) that for any $T \in SO(3)$,

$$M^{(1)}(TP, TP') = \int \boldsymbol{r} G(\boldsymbol{r}, TP, TP')\mathrm{d}\boldsymbol{r} = \int \boldsymbol{r} G(T^{-1}\boldsymbol{r}, P, P')\mathrm{d}\boldsymbol{r}$$
$$= \int (T\boldsymbol{r}) G(\boldsymbol{r}, P, P')\mathrm{d}\boldsymbol{r} = TM^{(1)}(P, P').$$

It implies that if we already know the value of $\tilde{c}_j(I, P^{-1}P)$, we may let $\tilde{c}_j(P, P') = \tilde{c}_j(I, P^{-1}P')$ in (2.14) to obtain a representation. From now on, we will omit this kind of explanation and just write

$$(2.18) \qquad \tilde{c}_j(TP, TP') = \tilde{c}_j(P, P') = \tilde{c}_j(I, P^{-1}P') \triangleq \tilde{c}_j(\bar{P}), \; j = 1, 2, 1', 2'.$$

Next, we substitute (P, P') with $(PJ, P'J)$ in (2.14). Using (2.10), we obtain

$$
\begin{aligned}
M^{(1)}(PJ, P'J) &= -M^{(1)}(P, P') \\
&= \tilde{c}_1(J\bar{P}J)(-\boldsymbol{m}_1) + \tilde{c}_2(J\bar{P}J)(-\boldsymbol{m}_2) + \tilde{c}_{1'}(J\bar{P}J)(-\boldsymbol{m}_1') + \tilde{c}_{2'}(J\bar{P}J)(-\boldsymbol{m}_2') \\
&= -\tilde{c}_1(\bar{P})\boldsymbol{m}_1 - \tilde{c}_2(\bar{P})\boldsymbol{m}_2 - \tilde{c}_{1'}(\bar{P})\boldsymbol{m}_1' - \tilde{c}_{2'}(\bar{P})\boldsymbol{m}_2',
\end{aligned}
$$

yielding (cf. (2.11))

$$
(2.19) \qquad \tilde{c}_j(\bar{P}) = \tilde{c}_j(J\bar{P}J) \triangleq \tilde{c}_j(p_{11}, p_{12}, p_{21}, p_{22}), \ \ j = 1, 2, 1', 2'.
$$

At this point, we have eliminated the appearance of $\boldsymbol{m}_3$ and $\boldsymbol{m}_3'$ in (2.14). Then, we switch P and P' in (2.14). By (2.9), we have

$$
\begin{aligned}
M^{(1)}(P', P) &= -M^{(1)}(P, P') \\
&= \tilde{c}_1(\bar{P}^T)\boldsymbol{m}_1' + \tilde{c}_2(\bar{P}^T)\boldsymbol{m}_2' + \tilde{c}_{1'}(\bar{P}^T)\boldsymbol{m}_1 + \tilde{c}_{2'}(\bar{P}^T)\boldsymbol{m}_2 \\
&= -\tilde{c}_1(\bar{P})\boldsymbol{m}_1 - \tilde{c}_2(\bar{P})\boldsymbol{m}_2 - \tilde{c}_{1'}(\bar{P})\boldsymbol{m}_1' - \tilde{c}_{2'}(\bar{P})\boldsymbol{m}_2'.
\end{aligned}
$$

Thus, we have $\tilde{c}_1(\bar{P}) = -\tilde{c}_{1'}(\bar{P}^T)$ and $\tilde{c}_2(\bar{P}) = -\tilde{c}_{2'}(\bar{P}^T)$, leading to (cf. (2.12))

$$
\begin{aligned}
(2.20) \qquad \tilde{c}_1(p_{11}, p_{12}, p_{21}, p_{22}) &= -\tilde{c}_{1'}(p_{11}, p_{21}, p_{12}, p_{22}), \\
\tilde{c}_2(p_{11}, p_{12}, p_{21}, p_{22}) &= -\tilde{c}_{2'}(p_{11}, p_{21}, p_{12}, p_{22}).
\end{aligned}
$$

Step 3. With the symmetric properties (2.20), we write down the polynomial approximation of $\tilde{c}_j$ with attention to the $\boldsymbol{m}_2 \to -\boldsymbol{m}_2$ and $\boldsymbol{m}_2' \to -\boldsymbol{m}_2'$ symmetries. The degree of polynomial is chosen such that both $\boldsymbol{m}_i$ and $\boldsymbol{m}_i'$ are truncated at second order in (2.14). For example, the term $p_{21}\boldsymbol{m}_2$ can be rewritten as $(\boldsymbol{m}_2 \cdot \boldsymbol{m}_1')\boldsymbol{m}_2$, in which the order of $\boldsymbol{m}_2$ is two. As an example, we look into $\tilde{c}_2$. The $\boldsymbol{m}_2 \to -\boldsymbol{m}_2$ symmetry allows only one term ap_{21} in the polynomial approximation, where a is the coefficient. Similarly, in the polynomial approximation of $\tilde{c}_{2'}$, there is also only one term $a'p_{12}$. Then, we use (2.20) to arrive at $a = -a'$. In this way, the polynomial approximations are written as

$$
(2.21) \qquad \tilde{c}_1 = -c_{10} - c_{11}p_{11}, \quad \tilde{c}_{1'} = c_{10} + c_{11}p_{11}, \quad \tilde{c}_2 = -c_{12}p_{21}, \quad \tilde{c}_{2'} = c_{12}p_{12},
$$

where we denote the coefficients by c_{1j}. The first index of c_{1j} becomes one to indicate that they come from $M^{(1)}$. The coefficients c_{1j} are independent of P and P'.

The expansion of $M^{(2)}$ follows the same way as $M^{(1)}$ and is described briefly. We start from

$$
M^{(2)}(P, P') = \sum_{l_1, l_2 = 1, 2, 3} \tilde{c}_{l_1 l_2} \boldsymbol{m}_{l_1} \boldsymbol{m}_{l_2}.
$$

Then, we express $\boldsymbol{m}_3$ by a linear combination of $\boldsymbol{m}_1$, $\boldsymbol{m}_2$, $\boldsymbol{m}_1'$, and $\boldsymbol{m}_2'$ if $\boldsymbol{m}_3' \neq \pm\boldsymbol{m}_3$. In the case $\boldsymbol{m}_3' = \pm\boldsymbol{m}_3$, we use (2.16) to obtain $\tilde{c}_{13} = \tilde{c}_{23} = \tilde{c}_{31} = \tilde{c}_{32} = 0$ (cf. (2.17)) and utilize the equality $\boldsymbol{m}_3\boldsymbol{m}_3 = I - \boldsymbol{m}_1\boldsymbol{m}_1 - \boldsymbol{m}_2\boldsymbol{m}_2$ to take care of the term $\boldsymbol{m}_3\boldsymbol{m}_3$. In any of the above two cases, we are allowed to use the following representation that is symmetric about P and P':

$$
\begin{aligned}
(2.22) \qquad M^{(2)}(P, P') = \tilde{c}_{00'}I &+ \sum_{l_1, l_2 = 1, 2} \tilde{c}_{l_1 l_2} \boldsymbol{m}_{l_1} \boldsymbol{m}_{l_2} + \sum_{l_1', l_2' = 1', 2'} \tilde{c}_{l_1' l_2'} \boldsymbol{m}_{l_1}' \boldsymbol{m}_{l_2}' \\
&+ \sum_{l=1,2, l'=1',2'} \tilde{c}_{ll'}(\boldsymbol{m}_l\boldsymbol{m}_{l'}' + \boldsymbol{m}_{l'}'\boldsymbol{m}_l),
\end{aligned}
$$

where we require that

$$\tilde{c}_{l_1 l_2} = \tilde{c}_{l_2 l_1},\ \tilde{c}_{l_1' l_2'} = \tilde{c}_{l_2' l_1'}$$

because $M^{(2)}$ is symmetric. Repeating the derivation of (2.18) and (2.19) for $M^{(1)}$, we can deduce that $\tilde{c}_{j_1 j_2}$ are functions of $(p_{11}, p_{12}, p_{21}, p_{22})$. Then, by switching P and P' in (2.22) and using (2.9), we obtain (cf. (2.20))

$$\begin{aligned}
(2.23) \qquad \tilde{c}_{00'}(p_{11}, p_{12}, p_{21}, p_{22}) &= \tilde{c}_{00'}(p_{11}, p_{21}, p_{12}, p_{22}), \\
\tilde{c}_{11}(p_{11}, p_{12}, p_{21}, p_{22}) &= \tilde{c}_{1'1'}(p_{11}, p_{21}, p_{12}, p_{22}), \\
\tilde{c}_{12}(p_{11}, p_{12}, p_{21}, p_{22}) &= \tilde{c}_{1'2'}(p_{11}, p_{21}, p_{12}, p_{22}), \\
\tilde{c}_{22}(p_{11}, p_{12}, p_{21}, p_{22}) &= \tilde{c}_{2'2'}(p_{11}, p_{21}, p_{12}, p_{22}), \\
\tilde{c}_{12'}(p_{11}, p_{12}, p_{21}, p_{22}) &= \tilde{c}_{21'}(p_{11}, p_{21}, p_{12}, p_{22}).
\end{aligned}$$

By noting the $\boldsymbol{m}_2 \to -\boldsymbol{m}_2$ and $\boldsymbol{m}_2' \to -\boldsymbol{m}_2'$ symmetries and keeping the truncation at second order for both $\boldsymbol{m}_i$ and $\boldsymbol{m}_i'$ in (2.22), we obtain the polynomial approximations of $\tilde{c}_{j_1 j_2}$,

$$\begin{aligned}
(2.24) \qquad \tilde{c}_{00'} &= -c_{20} - c_{21}p_{11} - c_{22}p_{11}^2 - c_{23}p_{22}^2 - c_{24}(p_{12}^2 + p_{21}^2), \\
\tilde{c}_{11} &= \tilde{c}_{1'1'} = -c_{25}, \\
\tilde{c}_{22} &= \tilde{c}_{2'2'} = -c_{26}, \\
\tilde{c}_{11'} &= -c_{27} - c_{28}p_{11}, \\
\tilde{c}_{22'} &= -c_{29}p_{22}, \\
\tilde{c}_{12} &= \tilde{c}_{21} = \tilde{c}_{1'2'} = \tilde{c}_{2'1'} = 0, \\
\tilde{c}_{12'} &= -c_{2,10}p_{12}, \quad \tilde{c}_{21'} = -c_{2,10}p_{21}.
\end{aligned}$$

Just as the notation for $M^{(0)}$ and $M^{(1)}$, the first index of c_{2j} is two. Again the coefficients c_{2j} do not depend on P and P'.

Summarizing (2.13), (2.14), (2.21), (2.22), and (2.24), we obtain the expansion of $M^{(0)}$, $M^{(1)}$, $M^{(2)}$, denoted by $\hat{M}^{(0)}$, $\hat{M}^{(1)}$, $\hat{M}^{(2)}$:

$$\begin{aligned}
(2.25) \qquad \hat{M}^{(0)} &= c_{00} + c_{01}p_{11} + c_{02}p_{11}^2 + c_{03}p_{22}^2 + c_{04}(p_{12}^2 + p_{21}^2), \\
\hat{M}^{(1)} &= (-c_{10} - c_{11}p_{11})(\boldsymbol{m}_1 - \boldsymbol{m}_1') - c_{12}(p_{21}\boldsymbol{m}_2 - p_{12}\boldsymbol{m}_2'), \\
\hat{M}^{(2)} &= -\big(c_{20} + c_{21}p_{11} + c_{22}p_{11}^2 + c_{23}p_{22}^2 + c_{24}(p_{12}^2 + p_{21}^2)\big)I \\
&\quad - c_{25}(\boldsymbol{m}_1\boldsymbol{m}_1 + \boldsymbol{m}_1'\boldsymbol{m}_1') - c_{26}(\boldsymbol{m}_2\boldsymbol{m}_2 + \boldsymbol{m}_2'\boldsymbol{m}_2') \\
&\quad - (c_{27} + c_{28}p_{11})(\boldsymbol{m}_1\boldsymbol{m}_1' + \boldsymbol{m}_1'\boldsymbol{m}_1) \\
&\quad - c_{29}p_{22}(\boldsymbol{m}_2\boldsymbol{m}_2' + \boldsymbol{m}_2'\boldsymbol{m}_2) \\
&\quad - c_{2,10}\left[p_{12}(\boldsymbol{m}_1\boldsymbol{m}_2' + \boldsymbol{m}_2'\boldsymbol{m}_1) + p_{21}(\boldsymbol{m}_2\boldsymbol{m}_1' + \boldsymbol{m}_1'\boldsymbol{m}_2)\right].
\end{aligned}$$

We substitute $M^{(k)}$ with $\hat{M}^{(k)}$ in (2.3). The purpose is to separate the variables P and P'. In this way, each term in $\hat{M}^{(k)}$ corresponds to a term in the free energy. Moreover, each term can be expressed by three tensors $\boldsymbol{p}$, Q_1, Q_2, defined as

$$(2.26) \qquad \boldsymbol{p} = \langle \boldsymbol{m}_1 \rangle,\ Q_1 = \langle \boldsymbol{m}_1 \boldsymbol{m}_1 \rangle,\ Q_2 = \langle \boldsymbol{m}_2 \boldsymbol{m}_2 \rangle,$$

where $\langle \cdot \rangle = \int \mathrm{d}P(\cdot)\rho(P)$ denotes the average about the orientational density ρ. As

an example, the term $-p_{12}^2 I$ in $\hat{M}^{(2)}$ generates the term $\nabla(cQ_1) : \nabla(cQ_2)$,

$$(2.27) \quad \int \mathrm{d}\boldsymbol{x}\mathrm{d}P\mathrm{d}P' - p_{12}^2 I : f(\boldsymbol{x}, P)\nabla^2 f(\boldsymbol{x}, P')$$

$$= -\int \mathrm{d}\boldsymbol{x} \left(c(\boldsymbol{x}) \int \mathrm{d}P m_{1i}m_{1j}\rho(\boldsymbol{x}, P) \right) \partial_{kk} \left(c(\boldsymbol{x}) \int \mathrm{d}P' m'_{2i}m'_{2j}\rho(\boldsymbol{x}, P') \right)$$

$$= -\int \mathrm{d}\boldsymbol{x} \left(c(\boldsymbol{x}) \langle m_{1i}m_{1j}\rangle \right) \partial_{kk} \left(c(\boldsymbol{x}) \langle m_{2i}m_{2j}\rangle \right),$$

$$= \int \mathrm{d}\boldsymbol{x}\partial_k \left(c(\boldsymbol{x})Q_{1ij} \right) \partial_k \left(c(\boldsymbol{x})Q_{2ij} \right).$$

Here we have done integration by parts and assume that the boundary terms vanish. We will write down all the terms afterwards in (2.35). One shall also observe that the three tensors are all the nontrivial tensors about $\boldsymbol{m}_1$ and $\boldsymbol{m}_2$ up to second order.

Finally, we point out that the derivation described in this section is applicable to any $M^{(k)}$, which is necessary if we aim to model smectic and columnar phases.

2.2.2. The entropy term. By the expansion discussed above, we have defined three tensors as order parameters. Now we can express the entropy term as a function of these tensors by a constrained minimization problem (cf. [2]). The entropy term can be rewritten as

$$\int \mathrm{d}\boldsymbol{x}\mathrm{d}P\, c\rho(\log c + \log \rho) = \int \mathrm{d}\boldsymbol{x} c \log c + \int \mathrm{d}\boldsymbol{x} \left(c(\boldsymbol{x}) \int \mathrm{d}P \rho \log \rho \right).$$

We minimize $\int \mathrm{d}P \rho \log \rho$ with the values of $\boldsymbol{p}$, Q_1, and Q_2 fixed. The Euler–Lagrange equation is written as

$$(2.28) \qquad 1 + \log \rho = \lambda + \boldsymbol{b} \cdot \boldsymbol{m}_1 + B_1 : \boldsymbol{m}_1\boldsymbol{m}_1 + B_2 : \boldsymbol{m}_2\boldsymbol{m}_2,$$

where the Lagrange multipliers are chosen such that

$$(2.29)$$
$$\int \mathrm{d}P\rho(P) = 1, \ \int \mathrm{d}P\boldsymbol{m}_1\rho(P) = \boldsymbol{p}, \ \int \mathrm{d}P\boldsymbol{m}_1\boldsymbol{m}_1\rho(P) = Q_1, \ \int \mathrm{d}P\boldsymbol{m}_2\boldsymbol{m}_2\rho(P) = Q_2.$$

The Euler–Lagrange equation gives the Boltzmann distribution,

$$(2.30) \qquad \rho = \frac{1}{Z}\exp(\boldsymbol{b} \cdot \boldsymbol{m}_1 + B_1 : \boldsymbol{m}_1\boldsymbol{m}_1 + B_2 : \boldsymbol{m}_2\boldsymbol{m}_2),$$

where Z is the normalization factor,

$$(2.31) \qquad Z = \int \mathrm{d}P\exp(\boldsymbol{b} \cdot \boldsymbol{m}_1 + B_1 : \boldsymbol{m}_1\boldsymbol{m}_1 + B_2 : \boldsymbol{m}_2\boldsymbol{m}_2).$$

We require that Q_1 and Q_2 share an eigenframe and that $\boldsymbol{p}$ be their eigenvector. This approximation comes from a theoretical result for homogeneous phases [36]. In other words, we assume that there exists a $T = (\boldsymbol{n}_1, \boldsymbol{n}_2, \boldsymbol{n}_3) \in SO(3)$ such that

$$(2.32)$$
$$\boldsymbol{p} = s\boldsymbol{n}_1, \ Q_1 = q_{11}\boldsymbol{n}_1\boldsymbol{n}_1 + q_{12}\boldsymbol{n}_2\boldsymbol{n}_2 + q_{13}\boldsymbol{n}_3\boldsymbol{n}_3, \ Q_2 = q_{21}\boldsymbol{n}_1\boldsymbol{n}_1 + q_{22}\boldsymbol{n}_2\boldsymbol{n}_2 + q_{23}\boldsymbol{n}_3\boldsymbol{n}_3,$$

with $q_{i3} = 1 - q_{i1} - q_{i2}$. The eigenvalues shall satisfy

$$(2.33) \qquad q_{ij} > 0, \ s^2 < q_{11},$$
$$q_{11} + q_{12}, q_{11} + q_{21}, q_{12} + q_{22}, q_{21} + q_{22} < 1,$$
$$q_{11} + q_{12} + q_{21} + q_{22} > 1.$$

They originate from $Q_1 - \boldsymbol{pp}$, Q_2, $I - Q_1 - Q_2$ being positive definite. Furthermore, if (s, q_{ij}) lies in a subregion given by the above constraints, there exists a unique $(\boldsymbol{b}, B_1, B_2)$ of the form

$$(2.34) \qquad \boldsymbol{b} = T(b_1, 0, 0)^T, \ B_1 = T\text{diag}(b_{11}, b_{12}, 0)T^T, \ B_2 = T\text{diag}(b_{21}, b_{22}, 0)T^T,$$

such that the moments of the corresponding Boltzmann distribution are $(\boldsymbol{p}, Q_1, Q_2)$. We state and prove the result rigorously in Appendix B (cf. Theorem B.1).

2.2.3. The free energy. Because we focus on nematic phases, we assume that $c(\boldsymbol{x}) = c_0$ is constant, still denoted as c. By (2.3), (2.25), (2.30) and integration by parts, the tensor model is written as follows:

$$(2.35) \quad \frac{F[\boldsymbol{p}, Q_1, Q_2]}{\beta_0} = \int \mathrm{d}\boldsymbol{x} \Big\{ c(\boldsymbol{b} \cdot \boldsymbol{p} + B_1 : Q_1 + B_2 : Q_2 - \log Z)$$
$$+ \frac{c^2}{2}(c_{01}|\boldsymbol{p}|^2 + c_{02}|Q_1|^2 + c_{03}|Q_2|^2 + 2c_{04}Q_1 : Q_2)$$
$$+ c^2(c_{11}p_j\partial_i Q_{1ij} + c_{12}p_j\partial_i Q_{2ij})$$
$$+ \frac{c^2}{4}\big[c_{21}|\nabla\boldsymbol{p}|^2 + c_{22}|\nabla Q_1|^2 + c_{23}|\nabla Q_2|^2 + 2c_{24}\partial_i Q_{1jk}\partial_i Q_{2jk}$$
$$+ 2c_{27}\partial_i p_i\partial_j p_j + 2c_{28}\partial_i Q_{1ik}\partial_j Q_{1jk}$$
$$+ 2c_{29}\partial_i Q_{2ik}\partial_j Q_{2jk} + 4c_{2,10}\partial_i Q_{1ik}\partial_j Q_{2jk}\big]\Big\},$$

where the components of $\boldsymbol{p}$ and Q_k are denoted as p_i and Q_{kij}. The first line comes from the entropy term. The second line comes from $\hat{M}^{(0)}$. The third line comes from $\hat{M}^{(1)}$, referred to as first-order elastic energy. They are crucial for modulated nematic phases to emerge. The rest of the terms come from $\hat{M}^{(2)}$, referred to as second-order elastic energy.

2.3. The coefficients. Now we describe how to calculate the coefficients in (2.35). We emphasize that the coefficients in the free energy are just those in $\hat{M}^{(k)}$. Note that $\hat{M}^{(k)}$ is the approximation of $M^{(k)}$ that is determined by molecular parameters. Hence we minimize the distance between $\hat{M}^{(k)}$ and $M^{(k)}$, defined as

$$(2.36) \qquad \int_{SO(3)} \mathrm{d}P\mathrm{d}P'||M^{(k)}(P, P'; l, D, \theta) - \hat{M}^{(k)}(P, P'; \{c_{kj}\})||_F^2,$$

where $|| \cdot ||_F$ is the Frobenius norm $||M||_F^2 = \sum_{i_1 \ldots i_k} |M_{i_1 \ldots i_k}|^2$. By solving this linear least-square problem, we can express c_{kj} as functions of the molecular parameters l, D, and θ. Furthermore, we have $c_{kj} \propto l^{k+3}$ because $M^{(k)}$ has the same scaling. Therefore, we can further nondimensionalize the model by the substitution $\bar{\boldsymbol{x}} = \boldsymbol{x}/l$, $\bar{c} = cl^3$, $\bar{c}_{kj} = c_{kj}/l^{k+3}$. Now $\bar{c}_{kj}$ become functions of two dimensionless parameters $\eta = D/l$ and θ. For star molecules, $\hat{M}^{(k)}$ also depends on l_2, and thus $\bar{c}_{kj}$ are also functions of l_2/l. For convenience, we still express these dimensionless quantities by the original notation.

The second-order elastic energy shall be positive definite to ensure the lower boundedness of the free energy. This can be guaranteed if the following inequalities hold:

$$(2.37) \qquad c_{21}, c_{22}, c_{23}, 2c_{27} + c_{21}, 2c_{28} + c_{22}, 2c_{29} + c_{23} \geq 0,$$
$$c_{24}^2 \leq c_{22}c_{23},$$
$$(2c_{2,10} + c_{24})^2 \leq (2c_{28} + c_{22})(2c_{29} + c_{23}).$$

These inequalities can be easily observed after we rewrite the c_{2j} terms for $7 \leq j \leq 10$, for which we explain by the term c_{27}. First, we observe that $\partial_i p_i \partial_j p_j - \partial_j p_i \partial_i p_j$ is a boundary term. Thus, we can substitute $\partial_i p_i \partial_j p_j$ with $\partial_j p_i \partial_i p_j$ by doing integration by parts and assume that the boundary term vanishes by adopting suitable boundary conditions (for example, periodic boundary conditions that will be used later). Then, we write

$$\partial_i p_j \partial_i p_j = \partial_i p_j \partial_j p_i + \frac{1}{2}|\partial_i p_j - \partial_j p_i|^2.$$

By doing the same thing to the other three terms, the second-order elastic energy becomes

$$\int \mathrm{d}\boldsymbol{x} \frac{c^2}{4} \left[\frac{1}{2}c_{21}|\partial_i p_j - \partial_j p_i|^2 + (2c_{27} + c_{21})(\partial_i p_i)^2 + \frac{1}{2}c_{22}|\partial_i Q_{1jk} - \partial_j Q_{1ik}|^2 \right.$$
$$+ \frac{1}{2}c_{23}|\partial_i Q_{2jk} - \partial_j Q_{2ik}|^2 + c_{24}(\partial_i Q_{1jk} - \partial_j Q_{1ik})(\partial_i Q_{2jk} - \partial_j Q_{2ik})$$
$$\left. + (2c_{28} + c_{22})|\partial_i Q_{1ik}|^2 + (2c_{29} + c_{23})|\partial_i Q_{2ik}|^2 + 2(2c_{2,10} + c_{24})\partial_i Q_{1ik}\partial_j(Q_{2jk}) \right].$$

Moreover, if $(2c_{2,10} + c_{24})^2 < (2c_{28} + c_{22})(2c_{29} + c_{23})$ or $c_{21} > 0$, it controls the first-order elastic energy. For example, we have

$$(2c_{28} + c_{22})|\partial_i Q_{1ik}|^2 + (2c_{29} + c_{23})|\partial_i Q_{2ik}|^2 + 2(2c_{2,10} + c_{24})\partial_i Q_{1ik}\partial_j(Q_{2jk})$$
$$- 4\partial_i p_j(c_{11}Q_{1ij} + c_{12}Q_{2ij}) \geq -C|\boldsymbol{p}|^2$$

for C large enough, and the right-hand side is bounded from below since $|\boldsymbol{p}| < 1$.

When $\theta = \pi$, the molecule becomes a rod. In this case, all the coefficients involving $\boldsymbol{p}$ and Q_1 shall be zero, which is verified in our numerical calculation. Furthermore, it can be shown with Theorem B.1 that in the entropy term we have $\boldsymbol{b} = B_1 = 0$, for which we omit the details. Thus, the free energy depends only on Q_2, written as

$$(2.38) \qquad \frac{F[Q_2]}{\beta_0} = \int \mathrm{d}\boldsymbol{x} \left\{ c(B_2 : Q_2 - \log Z) + \frac{c^2}{2}c_{03}|Q_2|^2 \right.$$
$$\left. + \frac{c^2}{4}\left(c_{23}|\nabla Q_2|^2 + 2c_{29}\partial_i Q_{2ik}\partial_j Q_{2jk}\right) \right\}.$$

It is a simplified version of the model proposed for rod-like molecules in [14] (see (3.15) in [14]), including only the terms involving the second-order tensor. The condition (2.37) becomes $c_{23}, 2c_{29} + c_{23} \geq 0$. It is weaker than what is proposed in [18] for rod-like molecules. This is because in [18], the derivatives of the tensors are viewed as independent functions, and the coercivity is assumed pointwise, which is a stronger condition than requiring the free energy to be lower bounded.
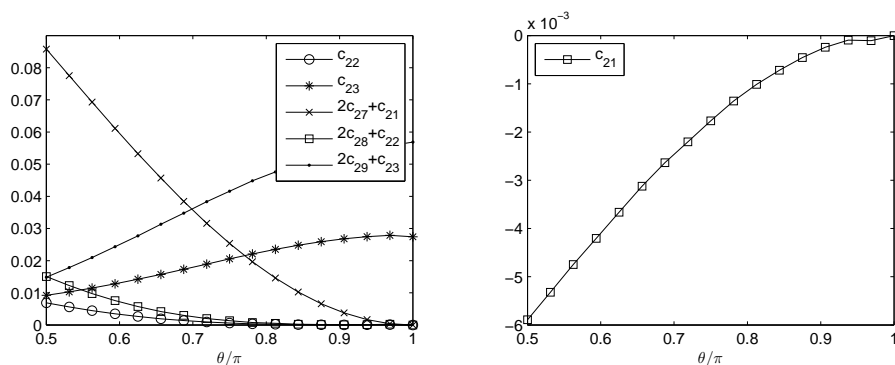
FIG. 2. *The coefficients c_{2j} in the second-order elastic energy for bent-core molecules, measured in the unit $(l/2)^5$, as functions of the bending angle θ when $\eta = 1/40$.*

Now we examine the coefficients calculated from (2.36). The coefficients of the square terms for bent-core molecules are plotted in Figure 2. When $\theta = \pi$, we have $c_{23}, 2c_{29} + c_{23} > 0$, and all the other c_{2j} are zero. As the bending angle decreases, c_{23} and $2c_{29} + c_{23}$ monotonely decrease, and the absolute values of other c_{2j} increase monotonely and thus do not change sign. We find that all of the inequalities in (2.37) hold strictly except $c_{21} < 0$. This is also the case for star molecules.

The signs of coefficients reflect a different modulation mechanism. The term $c_{21}|\nabla \boldsymbol{p}|^2$ can be stabilized if we truncate up to $M^{(4)}$. In fact, we write down the polynomial approximation $\hat{M}^{(4)}$ following the procedure described above, calculate the coefficients by (2.36), and find that the coefficient $c_{41} > 0$ for the corresponding term $c_{41}|\nabla^2 \boldsymbol{p}|^2$. The pair $c_{21}|\nabla \boldsymbol{p}|^2 + c_{41}|\nabla^2 \boldsymbol{p}|^2$ describes the tendency of independent modulation of $\boldsymbol{p}$ without coupling to Q_1 and Q_2. We can see this by taking the plane wave $\phi = \exp(i\boldsymbol{k} \cdot \boldsymbol{x})$ into the energy

$$\int \mathrm{d}\boldsymbol{x}|\nabla^2 \phi|^2 + 2K|\nabla \phi|^2 = (|\boldsymbol{k}|^4 + 2K|\boldsymbol{k}|^2)||\phi||^2.$$

If $K \geq 0$, the preferred frequency is $\boldsymbol{k} = 0$; if $K < 0$, the preferred frequency becomes $|\boldsymbol{k}| = \sqrt{-K} > 0$. On the contrary, the quadratic terms about ∇Q_1 and ∇Q_2 are positive, indicating that Q_1 and Q_2 do not tend to show independent modulation, but may show modulation coupled with $\boldsymbol{p}$ through the terms $p_i \partial_j Q_{\sigma ij}$. Currently, we choose not to include the independent modulation of $\boldsymbol{p}$ as an approximation, and we discard the term $c_{21}|\nabla \boldsymbol{p}|^2$ to avoid the lower unboundedness of the energy.

When we consider molecules with other shapes or interactions and calculate the coefficients from (2.36), we may obtain signs of the coefficients different from those above. If this is the case, it indicates that the molecular interaction induces a different modulation mechanism, and we need to do a different truncation in accordance with the mechanism.

3. Results and discussion. We examine the phases where inhomogeneity occurs only in the x-direction. To find modulated phases, we need to minimize the free energy density under the periodic boundary condition about the tensors and the period length L,

$$\min_{\boldsymbol{p}(x), Q_1(x), Q_2(x), L} \frac{F[\boldsymbol{p}(x), Q_1(x), Q_2(x)]}{L}.$$

3.1. Numerical methods. We use the finite volume method to discretize the free energy. Generally, in $[x_k, x_{k+1}]$, a function $g(x)$ is approximated by $\frac{1}{2}(g(x_k) + g(x_{k+1}))$, and its derivative is approximated by $(g(x_{k+1}) - g(x_k))/(x_{k+1} - x_k)$. For example, the term

$$\int_{x_k}^{x_{k+1}} \mathrm{d}x p_i \frac{\mathrm{d}}{\mathrm{d}x} Q_{1,1i}$$

is approximated by

$$(x_{k+1} - x_k) \cdot \frac{p_i(x_{k+1}) + p_i(x_k)}{2} \cdot \frac{Q_{1,1i}(x_k) - Q_{1,1i}(x_{k+1})}{x_{k+1} - x_k}.$$

A single period is discretized using 32 points. The tensors are represented by their eigenvalues and co-owned eigenframe $T(x)$, which is represented by the Euler angles $(\alpha(x), \beta(x), \gamma(x))$ by (2.1),

$$\boldsymbol{p}(x) = T(x)(s(x), 0, 0)^T,$$
$$Q_1(x) = T(x)\mathrm{diag}(q_{11}(x), q_{12}(x), q_{13}(x))T(x)^T,$$
$$Q_2(x) = T(x)\mathrm{diag}(q_{21}(x), q_{22}(x), q_{23}(x))T(x)^T.$$

The eigenvalues are calculated from (b_1, b_{ij}) using (2.30) and (2.34). We will use $(b_1(x), b_{ij}(x))$ and the Euler angles as the basic variables.

The derivatives of the free energy about the eigenvalues are given by

(3.1) $$\frac{\partial F}{\partial q_{ij}(x)} = b_{ij}(x) + \frac{\partial F_r}{\partial q_{ij}(x)}.$$

Here F_r stands for the part of free energy from the pairwise interaction, and the derivatives of the entropy term are calculated by (B.3). The derivatives about the Euler angles are given by

$$\frac{\partial F}{\partial \alpha(x)} = \frac{\partial F_r}{\partial \alpha(x)}$$

since the entropy term is independent of $T(x)$. We use the following stationary point iteration:

(3.2) $$b_{ij}^{(k+1)}(x) = b_{ij}^{(k)}(x) - \lambda \frac{\partial F}{\partial q_{ij}^{(k)}(x)} = (1 - \lambda)b_{ij}^{(k)}(x) - \lambda \frac{\partial F_r}{\partial q_{ij}^{(k)}(x)},$$

(3.3) $$\alpha^{(k+1)}(x) = \alpha^{(k)}(x) - \mu \frac{\partial F_r}{\partial \alpha^{(k)}(x)}.$$

The iteration is along a descending direction of the free energy (see (B.6)).

The free energy density may have several local minima. Various initial guesses are adopted to obtain as many metastable phases as possible, including but not limited to all the phases presented in the current work. Then, we compare free energy density of each metastable phase and label the minimum one as the stable phase. In seeking metastable phases, we have also tried with phenomenological coefficients. It turns out that many phases can be stable under phenomenological coefficients, but they are found unstable or only metastable under coefficients derived from the hard-core potential. In this paper, we only report the stable phases under coefficients derived from the hard-core potential and leave other metastable phases to a future work.
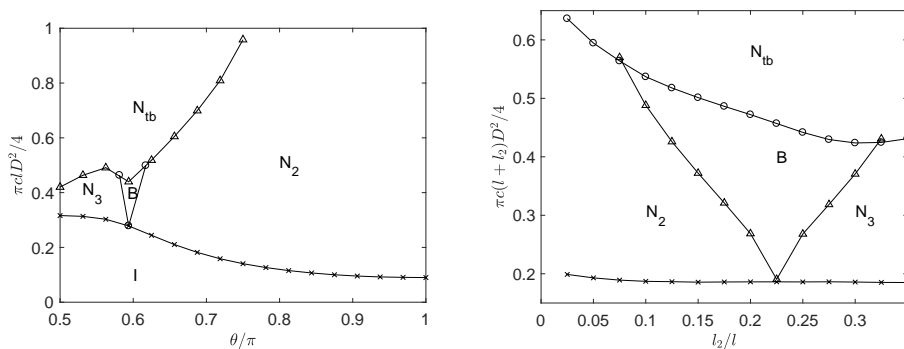
FIG. 3. *Left: phase diagram of bent-core molecules with* $\eta = D/l = 1/40$. *Right: phase diagram of star molecules with* $\theta = 2\pi/3$, $\eta = 1/40$.

3.2. The phase diagram. We first list the phases that appear in the phase diagram. Define $Q_3 = \langle \boldsymbol{m}_3 \boldsymbol{m}_3 \rangle = I - Q_1 - Q_2$, and denote its eigenvalues as q_{3j}. Because T is the eigenframe shared by Q_1 and Q_2, it is also the eigenframe of Q_3. For the phases discussed here, we can do permutation such that $q_{ii} \geq q_{ij}$ and assume this in the following. It should be noted that for homogeneous phases, the free energy is independent of the eigenframe T:

- Isotropic phase (I): $s = q_{ij} = 0$.
- Uniaxial nematic phase (N_i): homogeneous with $s = 0$ and further classified by the relation of the eigenvalues. In the N_2 phase, we have $q_{22} > 1/3 > q_{12}, q_{32}$ and $q_{j1} = q_{j3}$. In the N_3 phase, we have $q_{33} > 1/3 > q_{13}, q_{23}$ and $q_{j1} = q_{j2}$. The above relations of eigenvalues indicate that in the N_i phase, $\boldsymbol{m}_i$ aligns near $\pm \boldsymbol{n}_i$, and the other two $\boldsymbol{m}_j$ align near the plane perpendicular to $\boldsymbol{n}_i$.
- Biaxial nematic phase (B): homogeneous with $q_{ii} > q_{ij}$, indicating that $\boldsymbol{m}_i$ is preferably along $\pm \boldsymbol{n}_i$.
- Twist-bend phase (N_{tb}): the eigenvalues s and q_{ij} are constant with $s \neq 0$ and $q_{ii} > q_{ij}$, while $T(x)$ shows the modulation

(3.4)
$$T(x) = (\boldsymbol{n}_1, \boldsymbol{n}_2, \boldsymbol{n}_3) = \begin{pmatrix} 0 & -\cos\gamma & \sin\gamma \\ \cos\frac{\pm 2\pi x}{L} & -\sin\gamma \sin\frac{\pm 2\pi x}{L} & -\cos\gamma \sin\frac{\pm 2\pi x}{L} \\ \sin\frac{\pm 2\pi x}{L} & \sin\gamma \cos\frac{\pm 2\pi x}{L} & \cos\gamma \cos\frac{\pm 2\pi x}{L} \end{pmatrix},$$

where the modulation of $\boldsymbol{n}_2$ and $\boldsymbol{n}_3$ is identical to the earlier prediction [10]. The above equation indicates that $\boldsymbol{n}_1$ rotates on a circle and that $\boldsymbol{n}_2$ rotates on a conical surface. Thus, the Euler angle γ here becomes the conical angle. The sign before $2\pi x$ represents whether T is rotated left- or right-handed. The two cases share the same free energy density.

Although we only examine one-dimensional modulated phases, these phases have covered all the phases found experimentally so far.

The phase diagram of bent-core molecules is given in Figure 3(left), where we fix $\eta = 1/40$ and use the volume fraction $\pi c l D^2/4$ to express the concentration. It shows that I occurs at a low volume fraction, and homogeneous nematic phases emerge when it becomes higher. As the bending angle θ decreases from π, it shows successively N_2, B, and N_3. When the volume fraction further grows, the N_{tb} phase
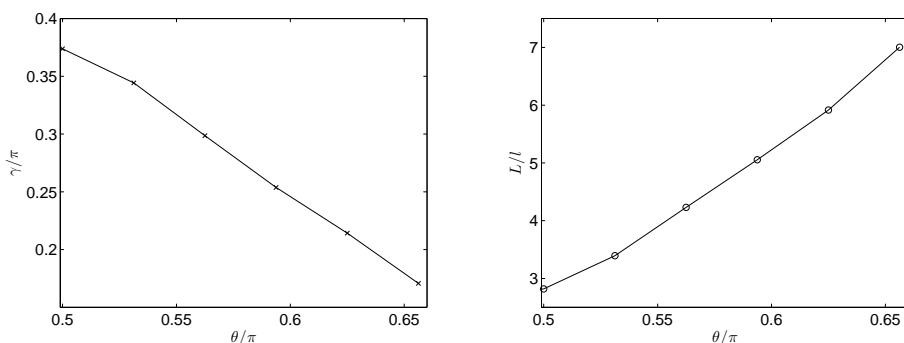
FIG. 4. *The conical angle γ and period length L as functions of the bending angle θ when* $\pi l D^2/4 = 0.7$.

occurs if the bending angle θ is far from π. Experimentally, the I–N_2–N_{tb} transition is also observed on lowering the temperature for molecules with relatively large bending angle θ [5, 7]. We also plot the conical angle γ and period length L as a function of θ at $\pi c l D^2/4 = 0.7$ (Figure 4). We observe that as θ increases, γ decreases while L increases. It is worth noting that L is a few times the dimension of the molecule, giving a very short periodicity that is consistent with the measurements of experiments [5, 7].

Next, we study the role of the third arm for star molecules. The phase diagram is presented in Figure 3(right). Here we fix the bending angle $\theta = 2\pi/3$ and focus on the length of the third arm l_2/l. Now the volume fraction becomes $\pi c(l + l_2)D^2/4$. The nematic phases are among those we mentioned above and are sensitive to l_2. While the transition volume fraction to homogeneous nematic phases is almost unchanged, the phase is altered from N_2 to B and to N_3 when l_2 increases. The transition volume fraction to N_{tb} is substantially lowered as l_2 grows. We would view this phase diagram as a typical example of phase behaviors being substantially altered by slight modification on molecular architecture. This is a feature different from rod-like molecules, commonly observed experimentally [31] but not yet well understood.

For bent-core molecules, the phase diagram about molecular parameters including modulated nematic phases has not to our knowledge been given in existing theoretical models. Moreover, in these models that focus on modulated phases, only one director $\boldsymbol{n}$ or one second-order tensor Q is included, leading to the absence of the biaxial phase B. The phase diagram about molecular parameters can only be found in preceding molecular simulations [6, 23, 17, 9, 25]. In these works, the molecules studied are thick with $\eta \approx 1/5 \sim 1/10$, and they did not find the N_{tb} phase. The results in [12] indicate that curved structure can make N_{tb} easier to occur. Our results suggest that thin molecules might have the same effect.

4. Conclusion. A tensor model is constructed based on molecular theory for nematic phases of bent-core molecules. The free energy is suitable for molecules with the C_{2v} symmetry, with the coefficients derived from molecular interaction. We use the model to study the nematic phases of bent-core molecules and their analogue, star molecules, with the hard-core potential. We obtain the phase diagram about the molecular parameters, including all the nematic phases found experimentally.

Provided that the molecular symmetry is preserved, the tensor model is able to study molecules with arbitrary shape and interactions. Hence we aim to apply this model to studying nematic phases of various molecules. We are also interested in two-
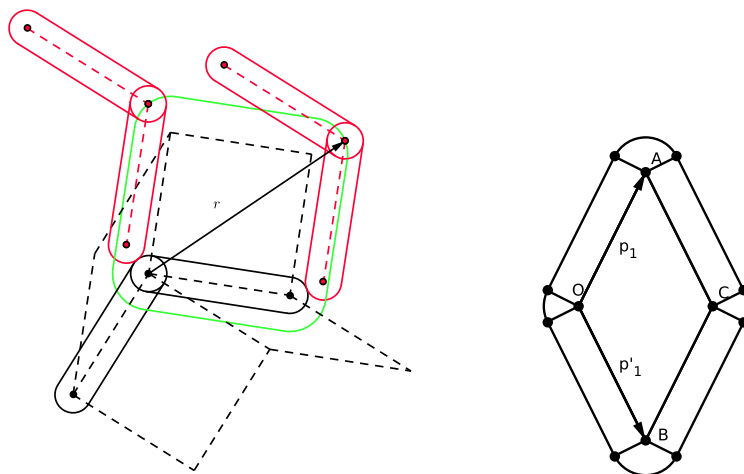
FIG. 5. *Left: the region W, consisting of four sphero-parallelograms, whose skeleton parallelograms are drawn with a dashed line. Right: the intersection of a sphero-parallelogram with the plane $z = 0$ in which the parallelogram lies.*

and three-dimensional modulated phases that can be described by the model.

Appendix A. The computation of $M^{(k)}$. We describe how to compute $M^{(k)}$ for bent-core molecules. It works exactly the same way for star molecules.

Fix the orientation of a pair of molecules. Denote by W_{ij} the region where the relative position lets the ith arm of one molecule and the jth arm of the other touch. Then, the region where two molecules touch, denoted by W, is the union of four W_{ij}. Each W_{ij} is a sphero-parallelogram, obtained by inflating each point in a parallelogram to a sphere. One of the W_{ij} is drawn in Figure 5(left). All four W_{ij} contain $\hat{O}$ since four arms share the point $\hat{O}$ when $\boldsymbol{r} = 0$.

Denote

$$s_{ij}(\boldsymbol{n}) = \max_{t\boldsymbol{n} \in W_{ij}} t.$$

Then,

$$\max_{t\boldsymbol{n} \in W} t \triangleq s(\boldsymbol{n}) = \max_{i,j=1,2} s_{ij}(\boldsymbol{n}).$$

For any vector $\boldsymbol{n}$, the whole segment $t\boldsymbol{n}$ ($t \in [0, s(\boldsymbol{n})]$) lies within W because W_{ij} are convex. Hence we can express $M^{(k)}$ by an integral in spherical coordinates, which we utilize for numerical calculation,

$$M^{(k)}(P, P') = \int_W \underbrace{\boldsymbol{r} \ldots \boldsymbol{r}}_{k \text{ times}} \mathrm{d}\boldsymbol{r} = \int_{S^2} \underbrace{\boldsymbol{n} \ldots \boldsymbol{n}}_{k \text{ times}} \mathrm{d}\boldsymbol{n} \int_0^{s(\boldsymbol{n})} r^{k+2} \mathrm{d}r$$

$$= \int_{S^2} \frac{1}{k+3} s(\boldsymbol{n})^{k+3} \underbrace{\boldsymbol{n} \ldots \boldsymbol{n}}_{k \text{ times}} \mathrm{d}\boldsymbol{n}.$$

Now it remains to compute s_{ij}. Place the parallelogram in the plane $z = 0$. Denote by R the intersection point of the ray $t\boldsymbol{n}$ ($t \geq 0$) and the boundary of the sphero-parallelogram. The boundary of a sphero-parallelogram consists of two planes $z = \pm D$, four cylindrical surfaces at four edges, and four spherical surfaces at four vertices. We need to determine where R lies, for which the procedure below is followed:

- Compute the intersection point of the ray $t\boldsymbol{n}$ and the plane $z = \pm D$. Then, examine whether its projection on the plane $z = 0$ lies in the parallelogram $OACB$, drawn in Figure 5(right). If it does, R lies on the flat surface of the sphero-parallelogram.
- Determine whether the ray $t\boldsymbol{n}$ intersects with any of the spheres on the corner. If yes, compute the farthest intersection point and examine its projection on the plane $z = 0$. If it lies in the corresponding sector (located at the corners in Figure 5), R lies on the spherical surface of the sphero-parallelogram.
- Now we know that R lies on the cylindrical surface of the sphero-parallelogram, and it is easy to distinguish which cylinder it locates.

Appendix B. The properties of the Boltzmann distribution.

B.1. The existence of the Lagrange multiplier. Let

$$\mathcal{A} = \left\{ (s, q_{ij}) | \rho : SO(3) \to \mathbb{R}^+, \ \int \mathrm{d}P\rho = 1, \ s = \int \mathrm{d}P\rho m_{11}, \ q_{ij} = \int \mathrm{d}P\rho m_{ij}^2, \ i, j = 1, 2 \right\}.$$

THEOREM B.1. *Each $(s, q_{ij}) \in \mathcal{A}$ is subject to the constraints in (2.33). For any (s, q_{ij}) satisfying (2.33), with $s^2 < q_{11}$ substituted by $s < q_{11}$, there exists a unique solution to the minimization problem*

$$\inf \int_{SO(3)} \mathrm{d}P\rho(P) \log \rho(P)$$

$$s.t. \ \int \mathrm{d}P\rho(P) = 1,$$

$$\int \mathrm{d}P\boldsymbol{m}_1\rho(P) = (s, 0, 0)^T,$$

$$\int \mathrm{d}P\boldsymbol{m}_1\boldsymbol{m}_1\rho(P) = \mathrm{diag}(q_{11}, q_{12}, 1 - q_{11} - q_{12}),$$

$$\int \mathrm{d}P\boldsymbol{m}_2\boldsymbol{m}_2\rho(P) = \mathrm{diag}(q_{21}, q_{22}, 1 - q_{21} - q_{22}).$$

The solution takes the form

$$\rho(P) = \frac{1}{Z} \exp\left(b_1 m_{11} + \sum_{i,j=1,2} b_{ij} m_{ij}^2 \right),$$

where

$$Z = \int \mathrm{d}P \exp\left(b_1 m_{11} + \sum_{i,j=1,2} b_{ij} m_{ij}^2 \right).$$

Proof. Note that

$$m_{13}^2 = 1 - m_{11}^2 - m_{12}^2 \geq 0,$$
$$m_{23}^2 = 1 - m_{21}^2 - m_{22}^2 \geq 0,$$
$$m_{31}^2 = 1 - m_{11}^2 - m_{21}^2 \geq 0,$$
$$m_{32}^2 = 1 - m_{12}^2 - m_{22}^2 \geq 0,$$
$$m_{33}^2 = m_{11}^2 + m_{12}^2 + m_{11}^2 + m_{12}^2 - 1 \geq 0$$

and that for $i, j = 1, 2, 3$, the measure of the set $\{P : m_{ij} = 0\}$ is zero. Thus, the inequalities about only q_{ij} in (2.33) are obtained. The inequality about s in (2.33) comes from $(\int dPf m_{11})^2 \leq \int dPf m_{11}^2$, and the equality holds only if $f m_{11} = \lambda f$ holds for a constant λ, which implies that $f = 0$ for $m_{11} \neq \lambda$. Again we note that the measure of the set $\{P : m_{11} = \lambda\}$ is zero.

The uniqueness of f is deduced immediately from the strict convexity of $f \log f$ about f.

To prove the existence, consider the function

$$(B.1) \qquad J(b_1, b_{ij}) = \int dP \exp\left(b_1(m_{11} - s) + \sum_{i,j=1,2} b_{ij}(m_{ij}^2 - q_{ij}) \right).$$

A stationary point of J satisfies $\partial J/\partial b_1 = \partial J/\partial b_{ij} = 0$, which yields

$$s = \frac{1}{Z} \int dP \exp\left(b_1 m_{11} + \sum_{i,j=1,2} b_{ij} m_{ij}^2 \right) m_{11},$$

$$q_{ij} = \frac{1}{Z} \int dP \exp\left(b_1 m_{11} + \sum_{i,j=1,2} b_{ij} m_{ij}^2 \right) m_{ij}^2, \quad i, j = 1, 2.$$

Because of the uniqueness, the stationary point of J solves the minimization problem. We will prove that

$$(B.2) \qquad \lim_{b_1^2 + \sum b_{ij}^2 \to \infty} J = +\infty.$$

Since J is bounded from below, (B.2) indicates the existence of a minimizer.

For (B.2), it is sufficient to prove that for any

$$(b_1, b_{11}, b_{12}, b_{21}, b_{22}) \neq (0, 0, 0, 0, 0),$$

there exists a P such that

$$I(P) = b_1(m_{11} - s) + \sum_{i,j=1,2} b_{ij}(m_{ij}^2 - q_{ij}) > 0.$$

Let

$$P_1 = \begin{pmatrix} 1 & 0 & 0 \\ 0 & 0 & 1 \\ 0 & -1 & 0 \end{pmatrix}, \qquad P_2 = \begin{pmatrix} -1 & 0 & 0 \\ 0 & 0 & 1 \\ 0 & 1 & 0 \end{pmatrix},$$

$$P_3 = \begin{pmatrix} 1 & 0 & 0 \\ 0 & 1 & 0 \\ 0 & 0 & 1 \end{pmatrix}, \qquad P_4 = \begin{pmatrix} -1 & 0 & 0 \\ 0 & 1 & 0 \\ 0 & 0 & -1 \end{pmatrix},$$

$$P_5 = \begin{pmatrix} 0 & 1 & 0 \\ 0 & 0 & 1 \\ 1 & 0 & 0 \end{pmatrix}, \qquad P_6 = \begin{pmatrix} 0 & 0 & 1 \\ 1 & 0 & 0 \\ 0 & 1 & 0 \end{pmatrix},$$

$$P_7 = \begin{pmatrix} 0 & 0 & -1 \\ 0 & 1 & 0 \\ 1 & 0 & 0 \end{pmatrix}, \qquad P_8 = \begin{pmatrix} 0 & 1 & 0 \\ 1 & 0 & 0 \\ 0 & 0 & -1 \end{pmatrix}.$$

It is straightforward to verify that

$$\lambda_i I(P_i) = 0$$

holds for arbitrary (b_1, b_{ij}), where

$$\lambda_1 = (\lambda - q_{22}) \left(\frac{1}{2} + \frac{s}{2q_{11}} \right), \qquad \lambda_2 = (\lambda - q_{22}) \left(\frac{1}{2} - \frac{s}{2q_{11}} \right),$$

$$\lambda_3 = (q_{11} + q_{22} - \lambda) \left(\frac{1}{2} + \frac{s}{2q_{11}} \right), \qquad \lambda_4 = (q_{11} + q_{22} - \lambda) \left(\frac{1}{2} - \frac{s}{2q_{11}} \right),$$

$$\lambda_5 = 1 - \lambda - q_{12}, \qquad \lambda_6 = 1 - \lambda - q_{21},$$

$$\lambda_7 = \lambda - q_{11}, \qquad \lambda_8 = q_{12} + q_{21} - (1 - \lambda).$$

Here λ is a real number to be determined. We choose a λ such that $\lambda_i > 0$. It is equivalent to

$$\lambda - q_{22}, \ q_{11} + q_{22} - \lambda, \ \lambda - q_{11}, \ 1 - \lambda - q_{12}, \ 1 - \lambda - q_{21}, \ q_{21} + q_{12} - (1 - \lambda) > 0,$$

which yields

$$\max\{q_{11}, q_{22}, 1 - q_{12} - q_{21}\} < \lambda < \min\{1 - q_{12}, 1 - q_{21}, q_{11} + q_{22}\}.$$

From the constraints on q_{ij}, the upper bound is greater than the lower bound, which guarantees the existence of λ. Note that

$$\sum_{i=1}^{8} \lambda_i = 1.$$

Let

$$A = b_1 s + \sum_{i,j=1,2} b_{ij} q_{ij}.$$

We claim that $I(P_i) > 0$ for some i. Otherwise, $I(P_i) = 0$ for every i. Expanding these equalities, we have

$$\pm b_1 + b_{11} = \pm b_1 + b_{11} + b_{22} = b_{21} = b_{12} = b_{22} = b_{12} + b_{21} = A.$$

It is easy to deduce that $b_1 = b_{ij} = 0$. $\qquad \square$

B.2. Some equalities. The derivatives of $F_{entropy}$ about the tensors are

(B.3) $$\frac{1}{\beta_0} \frac{\partial F_{entropy}}{\partial (\boldsymbol{p}, Q_1, Q_2)} = (\boldsymbol{b}, B_1, B_2).$$

We prove it for $\boldsymbol{p}$ as an example. Note that

(B.4) $$\frac{\partial \log Z}{\partial (\boldsymbol{b}, B_1, B_2)} = \frac{1}{Z} \frac{\partial Z}{\partial (\boldsymbol{b}, B_1, B_2)} = (\boldsymbol{p}, Q_1, Q_2).$$

Hence

$$\frac{1}{\beta_0}\frac{\partial F_{entropy}}{\partial \boldsymbol{p}}$$

$$= \frac{\partial(\boldsymbol{b}\cdot\boldsymbol{p} + B_1 : Q_1 + B_2 : Q_2 - \log Z)}{\partial \boldsymbol{p}}$$

$$= \boldsymbol{b} + \boldsymbol{p}\cdot\frac{\partial \boldsymbol{b}}{\partial \boldsymbol{p}} + Q_1 : \frac{\partial B_1}{\partial \boldsymbol{p}} + Q_2 : \frac{\partial B_2}{\partial \boldsymbol{p}} - \frac{\partial \log Z}{\partial \boldsymbol{p}}$$

$$= \boldsymbol{b} + \frac{\partial \log Z}{\partial \boldsymbol{b}}\cdot\frac{\partial \boldsymbol{b}}{\partial \boldsymbol{p}} + \frac{\partial \log Z}{\partial B_1}:\frac{\partial B_1}{\partial \boldsymbol{p}} + \frac{\partial \log Z}{\partial B_2}:\frac{\partial B_2}{\partial \boldsymbol{p}} - \frac{\partial \log Z}{\partial \boldsymbol{p}}$$

$$= \boldsymbol{b} + \frac{\partial \log Z}{\partial(\boldsymbol{b}, B_1, B_2)}\cdot\frac{\partial(\boldsymbol{b}, B_1, B_2)}{\partial \boldsymbol{p}} - \frac{\partial \log Z}{\partial \boldsymbol{p}}$$

$$= \boldsymbol{b}.$$

The derivatives of F about $b_{ij}(x)$ can be written as

$$\text{(B.5)} \qquad \frac{\partial F}{\partial b_{ij}(x)} = \frac{\partial q_{kl}(x)}{\partial b_{ij}(x)}\frac{\partial F}{\partial q_{kl}(x)}.$$

And note that

$$\frac{\partial q_{kl}(x)}{\partial b_{ij}(x)} = \frac{\partial^2 Z}{\partial b_{ij}(x)\partial b_{kl}(x)} = \left\langle (m_{11}, m_{11}^2, m_{12}^2, m_{21}^2, m_{22}^2)^T (m_{11}, m_{11}^2, m_{12}^2, m_{21}^2, m_{22}^2)\right\rangle$$

is positive definite. Thus,

$$\text{(B.6)} \qquad \left(\frac{\partial F}{\partial b_{ij}(x)}\right)^T \frac{\partial F}{\partial q_{ij}(x)} = \left(\frac{\partial F}{\partial q_{ij}(x)}\right)^T \frac{\partial^2 Z}{\partial b_{ij}(x)\partial b_{kl}(x)}\frac{\partial F}{\partial q_{ij}(x)} > 0.$$

REFERENCES

[1] B. R. Acharya, A. Primak, and S. Kumar, *Biaxial nematic phase in bent-core thermotropic mesogens*, Phys. Rev. Lett., 92 (2004), 145506.

[2] J. M. Ball and A. Majumdar, *Nematic liquid crystals: From Maier-Saupe to a continuum theory*, Mol. Cryst. Liq. Cryst., 525 (2010), pp. 1–11.

[3] C. Bingham, *An antipodally symmetric distribution on the sphere*, Ann. Statist., 2 (1974), pp. 1201–1225.

[4] F. Bisi, E. G. Virga, E. C. Gartland, G. D. Matteis, A. M. Sonnet, and G. E. Durand, *Universal mean-field phase diagram for biaxial nematics obtained from a minimax principle*, Phys. Rev. E (3), 73 (2006), 051709.

[5] V. Borshch, Y.-K. Kim, J. Xiang, M. Gao, A. Jákli, V. P. Panov, J. K. Vij, C. T. Imrie, M. G. Tamba, G. H. Mehl, and O. D. Lavrentovich, *Nematic twist-bend phase with nanoscale modulation of molecular orientation*, Nat. Commun., 4 (2013), 2635.

[6] P. J. Camp, M. P. Allen, and A. J. Masters, *Theory and computer simulation of bent-core molecules*, J. Chem. Phys, 111 (1999), pp. 9871–9881.

[7] D. Chen, J. H. Porada, J. B. Hooper, A. Klittnick, Y. Shen, M. R. Tuchband, E. Korblova, D. Bedrov, D. M. Walba, M. A. Glaser, J. E. Maclennan, and N. A. Clark, *Chiral heliconical ground state of nanoscale pitch in a nematic liquid crystal of achiral molecular dimers*, Proc. Natl. Acad. Sci. USA, 110 (2013), pp. 15931–15936.

[8] D. A. Coleman, J. Fernsler, N. Chattham, M. Nataka, Y. Takanishi, E. Körblova, D. R. Link, R.-F. Shao, W. G. Jang, J. E. Maclennan, O. Mondainn-Monval, C. Boyer, W. Weissflog, G. Pelzl, L.-C. Chien, J. Zasadzinski, J. Watanabe, D. M. Walba, H. Takezoe, and N. A. Clark, *Polarization-modulated smectic liquid crystal phases*, Science, 301 (2003), pp. 1204–1211.

[9] A. Dewar and P. J. Camp, *Dipolar interactions, molecular flexibility, and flexoelectricity in bent-core liquid crystals*, J. Chem. Phys., 123 (2005), 174907.

[10] I. Dozov, *On the spontaneous symmetry breaking in the mesophases of achiral banana-shaped molecules*, Europhys. Lett., 56 (2001), pp. 247–253.

[11] A. Eremin, A. Nemeş, R. Stannarius, and W. Weissflog, *Ambidextrous bend patterns in free-standing polar smectic-CP_F films*, Phys. Rev. E (3), 78 (2008), 061705.

[12] C. Greco and A. Ferrarini, *Entropy-driven chiral order in a system of achiral bent particles*, Phys. Rev. Lett., 115 (2015), 147805.

[13] C. Greco, G. R. Luckhurst, and A. Ferrarini, *Molecular geometry, twist-bend nematic phase and unconventional elasticity: A generalised Maier–Saupe theory*, Soft Matter, 10 (2014), pp. 9318–9323.

[14] J. Han, Y. Luo, W. Wang, and P. Zhang, *From microscopic theory to macroscopic theory: A systematic study on modeling for liquid crystals*, Arch. Ration. Mech. Anal., 215 (2015), pp. 741–809.

[15] J. Katriel, G. Kventsel, G. Luckhurst, and T. Sluckin, *Free energies in the Landau and molecular field approaches*, Liq. Cryst., 1 (1986), pp. 337–355.

[16] H. Kusumaatmaja and A. Majumdar, *Free energy pathways of a multistable liquid crystal device*, Soft Matter, 11 (2015), pp. 4809–4817.

[17] Y. Lansac, P. K. Maiti, N. A. Clark, and M. A. Glaser, *Phase behavior of bent-core molecules*, Phys. Rev. E (3), 67 (2003), 011703.

[18] L. Longa, D. Monselesan, and H.-R. Trebin, *An extension of the Landau-Ginzburg-De Gennes theory for liquid crystals*, Liq. Cryst., 2 (1987), pp. 769–796.

[19] V. L. Lorman and B. Mettout, *Unconventional mesophases formed by condensed vector waves in a medium of achiral molecules*, Phys. Rev. Lett., 82 (1999), pp. 940–943.

[20] L. A. Madsen, T. J. Dingemans, M. Nakata, and E. T. Samulski, *Thermotropic biaxial nematic liquid crystals*, Phys. Rev. Lett., 92 (2004), 145505.

[21] J. E. Mayer and M. G. Mayer, *Statistical Mechanics*, John Wiley & Sons, New York, 1940.

[22] R. B. Mayer, *Structural problems in liquid crystal physics*, in Molecular Fluids (Les Houches Summer School in Theoretical Physics, 1973), R. Balian and G. Weil, eds., Gordon and Breach, New York, 1976, pp. 273–373.

[23] R. Memmer, *Liquid crystal phases of achiral banana-shaped molecules: A computer simulation study*, Liq. Cryst., 29 (2002), pp. 483–496.

[24] C. Meyer, G. R. Luckhurst, and I. Dozov, *Flexoelectrically driven electroclinic effect in the twist-bend nematic phase of achiral molecules with bent shapes*, Phys. Rev. Lett., 111 (2013), 067801.

[25] T. D. Nguyen, Z. Zhang, and S. C. Glotzer, *Molecular simulation study of self-assembly of tethered v-shaped nanoparticles*, J. Chem. Phys., 129 (2008), 244903.

[26] V. P. Panov, M. Nagaraj, J. K. Vij, Y. P. Panarin, A. Kohlmeier, M. G. Tamba, R. A. Lewis, and G. H. Mehl, *Spontaneous periodic deformations in nonchiral planar-aligned bimesogens with a nematic-nematic transition and a negative elastic constant*, Phys. Rev. Lett., 105 (2010), 167801.

[27] G. Pelzl, A. Eremin, S. Diele, H. Kresse, and W. Weissflog, *Spontaneous chiral ordering in the nematic phase of an achiral banana-shaped compound*, J. Mater. Chem, 12 (2002), pp. 2591–2593.

[28] M. Robinson, C. Luo, P. E. Farrell, R. Erban, and A. Majumdar, *From molecular to continuum modelling of bistable liquid crystal devices*, Liq. Cryst., 44 (2017), pp. 2267–2284.

[29] S. M. Shamid, D. W. Allender, and J. V. Selinger, *Predicting a polar analog of chiral blue phases in liquid crystals*, Phys. Rev. Lett., 113 (2014), 237801.

[30] S. M. Shamid, S. Dhakal, and J. V. Selinger, *Statistical mechanics of bend flexoelectricity and the twist-bend phase in bent-core liquid crystals*, Phys. Rev. E (3), 87 (2013), 052503.

[31] H. Takezoe and Y. Takanishi, *Bent-core liquid crystals: Their mysterious and attractive world*, Jpn. J. Appl. Phys., 45 (2006), pp. 597–625.

[32] W. Tomczyk, G. Pajak, and L. Longa, *Twist-bend nematic phases of bent-shaped biaxial molecules*, Soft Matter, 12 (2016), pp. 7445–7452.

[33] N. Vaupotič, M. Čepič, M. A. Osipov, and E. Gorecka, *Flexoelectricity in chiral nematic liquid crystals as a driving mechanism for the twist-bend and splay-bend modulated phases*, Phys. Rev. E (3), 89 (2014), 030501.

[34] E. G. Virga, *Double-well elastic theory for twist-bend nematic phases*, Phys. Rev. E (3), 89 (2014), 052502.

[35] J. Xu and P. Zhang, *From microscopic theory to macroscopic theory—symmetries and order parameters of rigid molecules*, Sci. China Math., 57 (2014), pp. 443–468.

[36] J. Xu and P. Zhang, *The transmission of symmetry in liquid crystals*, Commun. Math. Sci., 15 (2017), pp. 185–195.